



Cobaltite nanoparticles synthesis for improved fingerprint visualization on porous, semi-porous and non-porous surfaces

Vikash Bhadwa¹, Harshada Borude¹, Riya Raj¹, Sandeep Munjal^{1,*}

¹ Multidisciplinary Research & Innovation Centre, National Forensic Sciences University, Goa Campus, Ponda, Goa, India

[drsandeepmunjal@gmail.com] (Corresponding Author)*

Abstract

Fingerprints are one the most crucial evidences found at most of the crime scenes. Present article reports the synthesis of nickel cobaltite (NCO) nanoparticles using combustion method and their application for enhanced latent fingerprint (LFP) development on various surfaces. Phase purity of synthesized nanoparticles was confirmed by X-ray diffraction (XRD) studies. Synthesized NCO nanoparticles possess smaller crystallite size (~8nm). Due to this small crystallite size good clarity and fine details have been obtained in the developed fingerprints which allows to analyse up to third level classification. NCO nanoparticles were used for non-porous, semi-porous and porous surfaces to develop the latent fingerprints and have demonstrated superior fingerprint visualization and preservation. Current study also highlights the enhanced resolution of ridge characteristics and pore structure, paving the path to more accurate forensic fingerprint analysis. This paper also discussed and demonstrated that all the features of LFP are preserved in lifted fingerprints developed using NCO nanoparticle and also discussed the comparison of LFP features and characteristics developed using commercially used fingerprint powder and NCO nanoparticle. Detailed fingerprint analysis is performed using stereomicroscope of LFP developed on various surfaces for the measurement of average pore size, pore shape, pore density, density of NCO powder attached to sweat, minor details and ridge characteristics.

Keywords: *Latent Fingerprints, Nickel Cobaltite, Forensic Science, Nanoparticle, XRD, Cost-effective*

1. Introduction

The Fingerprints present on the fingers and thumb pads are a type of biometrics due to their uniqueness [1], which is formed by nearly parallel epidermal ridges and furrows [2]. The uniqueness and individual characteristics of fingerprint patterns arise from the different arrangement, shape, size, and number of minor details (ridge characteristics) in these patterns [3]. Due to their uniqueness, permanence, universal, and classifiable nature, fingerprints can be classified using various universally established

standard methods such as the Henry fingerprint classification system and the automated fingerprint identification system (AFIS) [4, 5].

Three main types of fingerprint patterns have been recognized, each with subtypes. The arch pattern, found in approximately 5-15% of the population, can be either a plain arch or a tented arch. The loop pattern, present in around 60-65% of the population, can be either a radial loop or an ulnar loop. The whorl pattern, seen in about 30-35% of the population, can be either a plain whorl, central pocket loop, double loop, or accidental, representing the class characteristics of fingerprints [6]. The loop and whorl patterns contain two innermost ridges termed type lines, which start parallel, diverge, and tend to surround an area known as the pattern area, which is essential in classification. The pattern area contains a point near or in front of the divergence of type lines called the delta. Additionally, minutiae such as bifurcation, trifurcation, bridge, ridge ending, dot, island, lake, hook, double bifurcation, opposed bifurcation, ridge crossing, opposed bifurcation/ridge ending, and the approximate centre of the fingerprint impression, termed the core, are crucial in fingerprint analysis [7].

Latent fingerprints (LFPs) can be deposited on various types of surfaces, such as porous, semi-porous, and non-porous surfaces, through the friction ridges of the finger impressions [8]. This deposition occurs due to the natural secretion of three main types of glands: eccrine glands, apocrine glands, and sebaceous glands, which are present beneath the skin to prevent it from becoming too dry. Although the palms of the hands contain a greater number of eccrine glands compared to apocrine and sebaceous glands [9], all three glands together are known as the sudoriferous glands, and their collective secretion is sweat [10]. Sweat contains approximately 99% water and 1% organic constituents such as amino acids, fatty acids, urea, lactic acid, and inorganic constituents like potassium, magnesium, calcium, sodium, and chloride [11].

Fingerprints are the most common type of physical evidence found at crime scenes and are widely accepted in criminal investigations and court proceedings for identifying an individual's identity [12]. They can establish a direct connection between the perpetrator or victim and the scene of the crime, making the development of LFPs necessary through suitable non-destructive techniques [13].

In forensic science, LFPs are developed using various methods, including dusting method, iodine fuming method, silver nitrate development, and ninhydrin treatment [14]. Each method has its own efficiency and application, depending on factors such as the type of surface (porous, semi-porous, or non-porous) on which the fingerprints are found, as well as factors like temperature, humidity, the pressure applied by the fingers, the age of the fingerprints, the dryness of the surface, and the secretory constituents of the eccrine, apocrine, and sebaceous glands [15]. Among all LFP development methods, powder dusting is one of the oldest, simplest, swiftest, and most effective techniques for developing LFPs on various types of dry surfaces [16]. The powder dusting technique is based on the cementing properties of the powder particles, which are highly influenced by the shape and size of the particles. It works by the mechanical binding of fingerprint powder to the moisture and oily content of the print residue [15].

Additionally, the appearance of LFPs developed using the powder dusting technique depends on various factors, such as temperature, humidity, age of the fingerprint, whether the surface was wet or dry, the type of surface (porous, semi-porous, or non-porous), the procedure and characteristics of the powder used (shape and size) [17]. All of the above methods of LFP development primarily help in studying the ridge characteristics of latent fingerprints, allowing fingerprint classification up to level two, which includes pattern type and ridge characteristics [18]. However, the use of nanoparticle-based fingerprint powder, which consists of solid particulates having dimension not more than 100 nm in any direction [19], significantly enhances the clarity of visualization of LFPs by revealing the pores present, enabling fingerprint classification at third level, includes pores and ridge shape (Poroscopy). This greatly increases the accuracy and efficiency of fingerprint classification and individualization [18]. As suggested by our previous study based on latent fingerprint development by using nanoparticles fingerprint powder [20,21].

The face-centred cubic crystalline structure [22] (inverse spinel structure) of nickel cobaltite (NCO) exhibits crystallographic symmetry, where octahedral voids are occupied by all nickel ions and half of the cobalt ions, and the remaining cobalt ions occupy tetrahedral voids [23]. NCO can be synthesized with various methods such as sol-gel, hydrothermal, solvothermal, electro-deposition, co-precipitation, combustion, electrospinning, Microwave-assisted, spray pyrolysis, template methods [24] and electrodeposition method [25]. For noble metals such as silver, gold, and palladium, NCO can be used as an effective alternative catalyst for the reduction of toxic pollutants and 4-nitrophenol [26]. Additionally, NCO nanomaterials can be utilized for supercapacitor [27] and biofuel applications [28]. They are cost-effective, making them an appealing choice for large-scale manufacturing.

2. Experimental Section

We synthesised Nickel Cobaltite nanoparticle using the combustion method, as it is well suited for bulk synthesis, cost-effective, and time-efficient.

2.1 Materials Required: I Cobalt (II) Nitrate Hexahydrate $\{\text{Co}(\text{NO}_3)_2 \cdot 6\text{H}_2\text{O}\}$, Nickle (II) Nitrate Hexahydrate $\{\text{Ni}(\text{NO}_3)_2 \cdot 6\text{H}_2\text{O}\}$, Citric Acid Anhydrous $\{\text{C}_6\text{H}_8\text{O}_7\}$, Ethanol $\{\text{C}_2\text{H}_5\text{OH}\}$. All the chemicals were used as purchased.

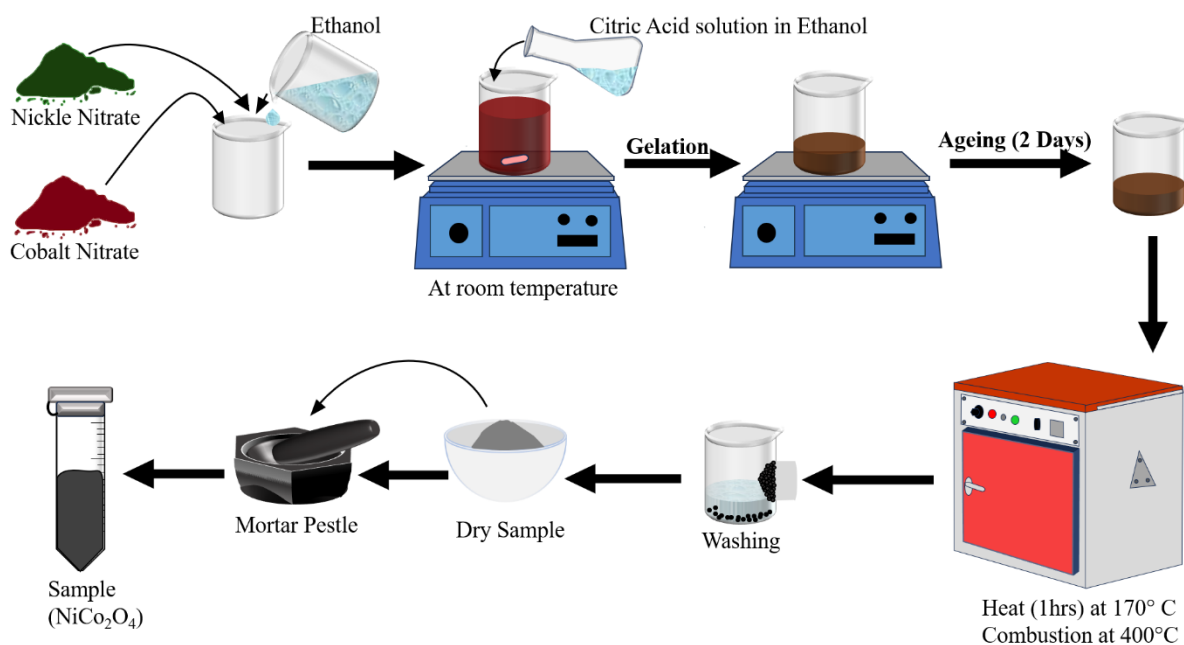


Figure 1. Schematic representation of Nickle Cobaltite nanoparticles synthesis.

2.2 Synthesis of Nickle Cobaltite Nanoparticle: Fig. 1 depicts the synthesis procedure of Nickel Cobaltite (NCO) nanoparticles. Initially, Cobalt (II) Nitrate Hexahydrate (0.021M) was dissolved in 20 ml of ethanol under stirring on a magnetic stirrer. Once fully dissolved, Nickel (II) Nitrate Hexahydrate (0.011M) was added to the Cobalt (II) Nitrate solution and stirred for 20 mins. In another beaker, a citric acid solution (0.031M) was prepared in 10 ml of ethanol, which was then added to the cobalt and nickel precursor solution and stirred for 5 hrs at room temperature to form a gel-like solution. After aging for 2 days, the solution was dried in a furnace at 170 °C for 1 hrs, followed by combustion at 400°C. The resulting

material was grinded using a mortar and pestle, then washed using distilled water. The material was left to dry and subsequently heated again at 200 °C to ensure complete drying. After this, the compound was grinded again using a mortar and pestle. The dried compound was then heated at 800 °C for 4 hrs. After cooling, the final product was grinded. XRD analysis later confirmed that the final product obtained was Nickel Cobaltite (NiCo_2O_4) nanoparticles ($\sim 0.009\text{M}$).

3. Result and Discussion

3.1 X-ray Diffraction analysis of NiCo_2O_4 : The XRD pattern of the synthesized material was recorded for diffraction angles (2θ) ranging from 20° to 70° using an X-ray diffractometer (Rigaku Ultima IV having Copper $\text{K}\alpha$ X-ray radiation of wavelength ($\text{Cu-K}\alpha \sim 1.542 \text{ \AA}$)). In the pattern obtained (shown in Fig. 2), diffraction peaks were observed at 2θ values of approximately 31.2° , 36.8° , 44.7° , 55.5° , 59.2° , and 65.1° , corresponding to the (220), (311), (400), (422), (511), and (440) Bragg's planes, respectively. These peaks indicate the formation of cubic spinel NCO. The peak positions and relative intensities of the obtained XRD pattern were matched with the standard reference data file JCPDS card no. 73-1702. No extra diffraction peaks were observed in the match, indicating the phase purity of the synthesized NCO nanoparticles with no noticeable impurities.

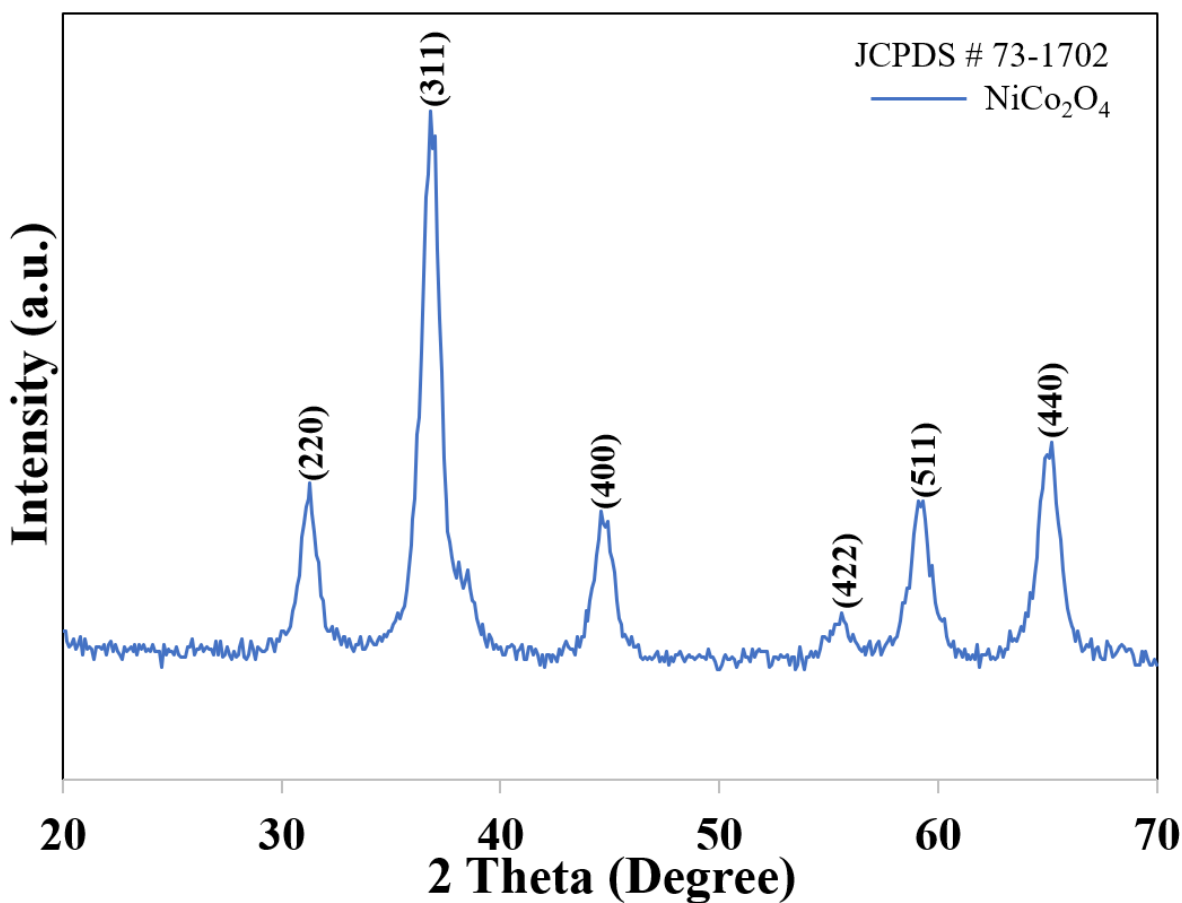


Figure 2. XRD Pattern of NiCo_2O_4 nanoparticle.

From the XRD data, the average crystallite size of the synthesized NCO nanoparticles was calculated using the Scherrer equation [29], as mentioned below:

$$D = k\lambda/\beta\cos\theta \quad (1)$$

Where D represents the average crystallite size of the synthesized nanoparticles, and k, λ , β , and θ represent the Scherrer constant, the wavelength of the X-ray beam used, the FWHM (full width at half maximum), and the Bragg's angle (diffraction angle) of the corresponding XRD peaks, respectively. Using the Scherrer constant ($k = 0.9$) and the wavelength of the X-ray beam ($\lambda \sim 0.154$ nm), the average crystallite size of the NCO nanoparticles was found to be approximately 8.4 nm.

3.2 Latent fingerprint development on non-porous and semi-porous surfaces: To determine the extent of clarity of visualization of LFP characteristics, LFPs were developed on non-porous surfaces, including glass slides, light-coloured painted surface, and whiteboard, as well as semi-porous surfaces, such as light-coloured wooden surfaces and rough wooden surfaces, using NCO nanoparticles. The surfaces were properly cleaned with an ethanol solution, and then fingerprints were deposited by lightly pressing the surface with thumbs and fingers. The latent fingerprints were developed by dusting black-coloured NCO nanoparticles powder (powder dusting method) [30] using a Technomaxx Forensics smooth brush. Excess powder was gently removed, and the results were photographed.

Among all the surfaces where LFPs were developed, the ridge flow and ridge quality were better on light-coloured painted metallic surfaces, whiteboards, glass slides, and wooden surfaces compared to glossy paper. The linear density of ridges was found to be approximately 2 ridges/mm. Due to the black colour of the NCO nanoparticles, the developed fingerprints provided good contrast against the light-coloured surfaces. In addition to the pattern type, all ridge characteristics (minor details) such as bifurcation, short ridges, dots, ridge endings, and bridges [31] were clearly visible with the naked eye in the photographs taken.

It was also observed that not only the pattern type and ridge characteristics were easily visible to the naked eye, but both types of pores were discernible as well. Closed pores, which were completely enclosed by the applied LFP development powder, and partially closed pores (open pores) [32], which were not fully enclosed by the powder at some points on their circumference, were visible in the photographs that can be attributed to the smaller crystallite size of NCO nanoparticles. This enhances the accuracy of fingerprint classification at all three levels: pattern type, ridge characteristics, and poroscopy [18]. Subsequently, the LFP developed on the painted metallic surface was tape lifted using standard fingerprint lifting tape and transferred onto a fingerprint card (Fig. 3 (b)) to assess the extent preservation of ridge characteristics. It was noted that the ridge flow, ridge quality, and all ridge characteristics, including minutiae, closed pores, and partially closed pores, were preserved in the lifted fingerprints. This indicates that the preservation of the LFP developed with NCO powder is easier and more reliable.

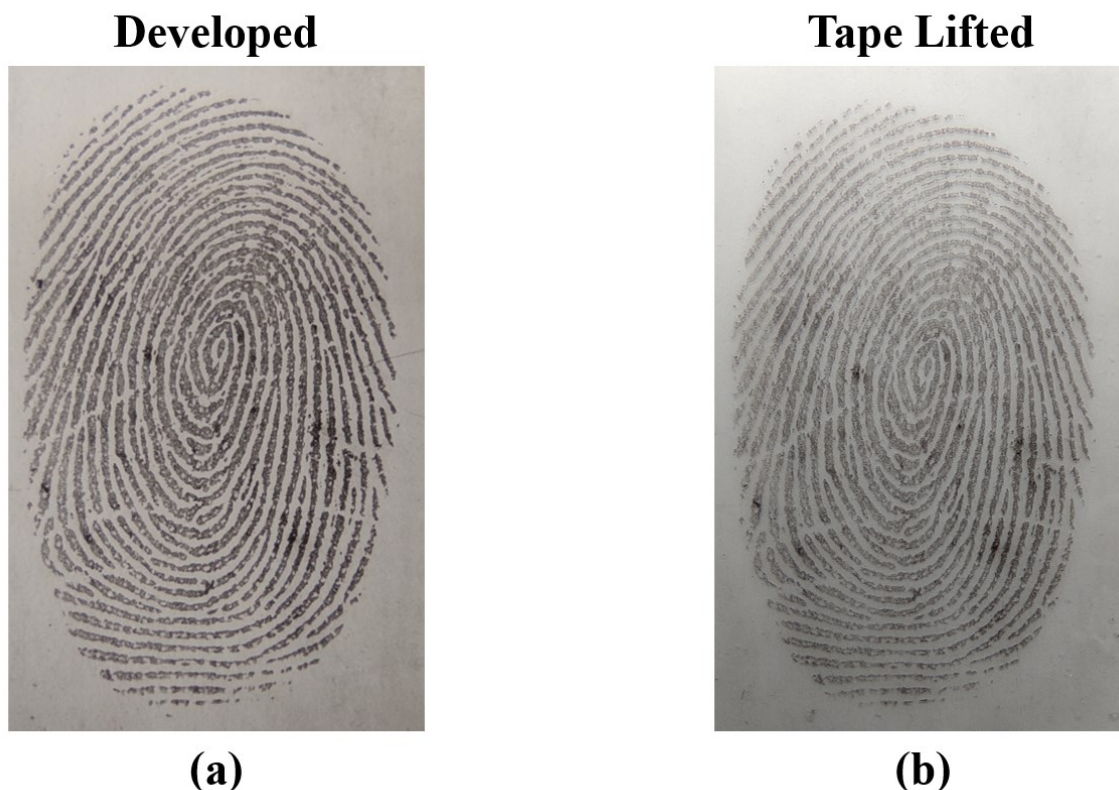


Figure 3. (a) Developed latent fingerprints on a light-coloured painted metallic surface by using NCO nanoparticles. (b) Tape lifted fingerprint with the standard fingerprint lifting tape on the fingerprint card by using NCO nanoparticles.

3.3 Development of latent fingerprint on porous surface: To determine the efficiency of the synthesized NCO nanoparticles compared to commercially used fingerprint powder, LFPs were developed on porous white-coloured paper using the NCO nanoparticles (Fig. 4 (a)) with the powder dusting method as previously described. Under similar conditions, LFPs were also developed using commercially available black magnetic latent fingerprint powder (Fig. 4 (b)) for comparison. The aspects compared included colour contrast against the white-coloured surface, ridge quality, smudging of the powder on the surface where fingerprints were developed, and the appearance of pores.

It was observed that fingerprints developed using the NCO nanoparticles provided better colour contrast without smudging the powder on the surface, compared to those developed with commercially used black magnetic fingerprint powder, where smudging occurred. These all-enhanced features can be attributed to smaller crystallite size of NCO nanoparticles. Additionally, the ridges appeared clearer in fingerprints developed with the NCO nanoparticles compared to those developed with commercially used black magnetic powder. This significantly enhanced the clarity of the ridge characteristics, core, delta, and appearance of pores in the fingerprints developed with NCO nanoparticles.



Figure 4. (a) Developed latent fingerprints on a white porous paper by using NCO nanoparticles. (b) Developed latent fingerprints on a white porous paper by using commercial black magnetic powder.

3.4 Detailed fingerprint analysis: LFPs were developed on non-porous surfaces (glass slides and glossy paper), semi-porous surfaces (smooth and rough wood), and porous surfaces (white paper) using black NCO nanoparticles powder, following the same method as previously described. The aim to conduct a detailed fingerprint analysis, includes the measurement of average pore size, pore shape, pore density, the density of NCO powder attached to sweat, minor details, and ridge characteristics, under a stereomicroscope [33] (Fig. 5). It was observed that the NCO nanoparticles adhered finely to the surface with the aid of the sweat present, with almost no smudging of the powder. Open and closed pores of various shapes, such as circular, oval, and irregular, along with ridge linings, were clearly visible in the LFPs developed using NCO nanoparticles. Radical ProCAM software was used to measure the diameter of closed and open pores by calculating the distance between two opposite points of the circular pores. It is evident that more than 50 pores are clearly visible and identifiable in the LFP developed on a glass slide under stereomicroscope as depicted in Fig. 5. As only 12 – 14 minutia points/ridge characteristics are required for matching [34]. Our developed fingerprint powder can be used as potential candidate for the development of latent fingerprints and to full fill the criteria setup by the various country's government and as per the ISO 19794-2 [35]. The diameters of 46 pores from LFPs on different surfaces were measured, revealing an average pore size of approximately 136.8 μm . A high pore density was observed under the stereomicroscope, calculated by the ratio of the number of pores per unit area [33]. This significantly enhanced the accuracy and precision of fingerprint classification based on poroscopy. Additionally, ridge characteristics such as bifurcation, short ridges, dots, ridge endings, and bridges were also clearly visible under the stereomicroscope, with a nearly identical ridge flow.

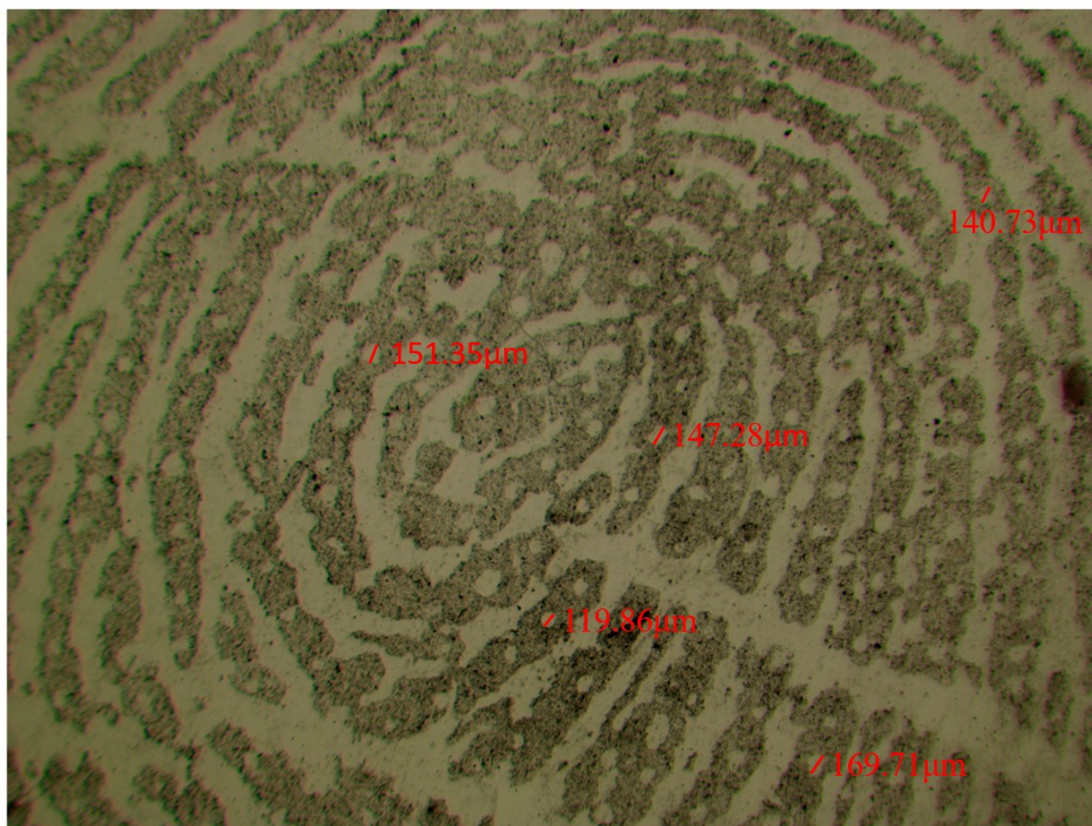


Figure 5. Pores of latent fingerprint developed on a glass slide under stereomicroscope.

4. Conclusion

In conclusion nickel cobaltite (NiCo_2O_4 , NCO) have been successfully synthesized and their potential in the development of latent fingerprints with enhanced visualization has been demonstrated. The latent fingerprints from various surfaces such as porous, semi-porous and non-porous have been developed. The developed fingerprints have been tape lifted for further preservation. Microscopic details of the developed fingerprint have been studied by performing level three analysis and measurement of average pore size, pore shape and pore density have been performed. Enhanced visualization of developed fingerprint characteristics may be attributed to smaller crystallite size of synthesized NCO nanoparticles. This study can pave the path of development of nano powders for latent fingerprint decipherment with optimum characteristics.

5. Acknowledgements

The authors are thankful to Multidisciplinary Research & Innovation Centre (MRIC), Forensic Physics Laboratory, fingerprint and Questioned Documents Laboratory, NFSU Goa Campus for their support and for providing their facilities, equipment's and chemicals for the synthesis and analysis process. The authors also acknowledge IIT Delhi NRF for material characterization. Finally, the authors extend their thanks to the NFSU Journal of Forensic Science editorial team for their support and guidance throughout the publication process.

References

- [1] W. Yang, S. Wang, J. Hu, G. Zheng, and C. Valli, "Security and Accuracy of Fingerprint-Based Biometrics: A Review," *Symmetry (Basel)*, vol. 11, no. 2, p. 141, Jan. 2019, doi: 10.3390/sym11020141.
- [2] M. Kücken and A. C. Newell, "Fingerprint formation," *J. Theor. Biol.*, vol. 235, no. 1, pp. 71–83, Jul. 2005, doi: 10.1016/j.jtbi.2004.12.020.
- [3] A. Ross, J. Shah, and A. K. Jain, "From Template to Image: Reconstructing Fingerprints from Minutiae Points," *IEEE Trans. Pattern Anal. Mach. Intell.*, vol. 29, no. 4, pp. 544–560, Apr. 2007, doi: 10.1109/TPAMI.2007.1018.
- [4] N. Kaushal and P. Kaushal, "Human Identification and Fingerprints: A Review," *J. Biom. Biostat.*, vol. 02, no. 04, 2011, doi: 10.4172/2155-6180.1000123.
- [5] N. Yager and A. Amin, "Fingerprint classification: a review," *Pattern Anal. Appl.*, vol. 7, no. 1, pp. 77–93, Apr. 2004, doi: 10.1007/s10044-004-0204-7.
- [6] A. Babich, "Biometric Authentication. Types of biometric identifiers," 2012.
- [7] C. Darwin, "The science of fingerprints: classification and uses," *Oxford Univ.*, vol. XXX, p. 60, 1895.
- [8] Y. D. Buzuayehu Abebe, Hanabe Chowdappa Ananda Murthy, Enyew Amare Zereffa, "Latent Fingerprint Enhancement Techniques: A Review," *J. Chem. Rev.*, vol. 2, no. 1, pp. 40–56, Jan. 2020, doi: 10.33945/SAMI/JCR.2020.1.3.
- [9] B. Su, "Recent progress on fingerprint visualization and analysis by imaging ridge residue components," *Anal. Bioanal. Chem.*, vol. 408, no. 11, pp. 2781–2791, Apr. 2016, doi: 10.1007/s00216-015-9216-y.
- [10] S. C. WAY, "THE SUDORIPAROUS GLANDS," *Arch. Derm. Syphilol.*, vol. 38, no. 3, p. 373, Sep. 1938, doi: 10.1001/archderm.1938.01480150047008.
- [11] G. McKnight, J. Shah, and R. Hargest, "Physiology of the skin," *Surg. (United Kingdom)*, vol. 40, no. 1, pp. 8–12, 2022, doi: 10.1016/j.mpsur.2021.11.005.
- [12] C. McCartney, *Forensic Identification and Criminal Justice*. Willan, 2013. doi: 10.4324/9781843926085.
- [13] A. Singh, V. Prasad, S. Lukose, and A. Kumar, "Silver and Gold Nanoparticles for the Development of Fingerprints," 2023, pp. 47–75. doi: 10.1007/978-981-99-4028-8_4.
- [14] K. Bashir et al., "From invisible to visible: a concise review on conjugated polymer materials in latent fingerprint analysis," *J. Polym. Res.*, vol. 31, no. 8, p. 235, Aug. 2024, doi: 10.1007/s10965-024-04086-1.
- [15] G. S. Sodhi and J. Kaur, "Powder method for detecting latent fingerprints: a review," *Forensic Sci. Int.*, vol. 120, no. 3, pp. 172–176, Sep. 2001, doi: 10.1016/S0379-0738(00)00465-5.
- [16] Z. Ben Qiu Zijie, Hao bin, Gu Xingguo, wang Zhaoyu, Xie Ni, W.Y.Lam Jacky, Hao Hongxia, "A general powder dusting method for latent fingerprint development based on AIEgens," 2018, doi: 10.1007/s11426-018-9280-1.
- [17] R. Rajan, Y. Zakaria, S. Shamsuddin, and N. F. N. Hassan, "Nanocarbon powder for latent fingermark development: a green chemistry approach," *Egypt. J. Forensic Sci.*, vol. 8, no. 1, p. 60, Dec. 2018, doi: 10.1186/s41935-018-0091-5.
- [18] A. Jain, Yi Chen, and M. Demirkus, "Pores and Ridges: Fingerprint Matching Using Level 3 Features," in

- 18th International Conference on Pattern Recognition (ICPR'06), IEEE, 2006, pp. 477–480. doi: 10.1109/ICPR.2006.938.
- [19] J. Jiang, G. Oberdörster, A. Elder, R. Gelein, P. Mercer, and P. Biswas, “Does nanoparticle activity depend upon size and crystal phase?,” *Nanotoxicology*, vol. 2, no. 1, pp. 33–42, Jan. 2008, doi: 10.1080/17435390701882478.
- [20] S. Rajan et al., “Synthesis of ZnO nanoparticles by precipitation method: Characterizations and applications in decipherment of latent fingerprints,” *Mater. Today Proc.*, Jun. 2023, doi: 10.1016/j.matpr.2023.05.680.
- [21] V. N. Halarnkar, A. S. Nair, D. Mandal, R. Kumar, and S. Munjal, “CoFe₂O₄ Based Black Magnetic Fingerprint Powder: Development, Analysis and Applications of Nanoparticles in Decipherment of Latent Fingerprints,” *NFSU J. FORENSIC Sci.*, vol. 1, no. 1, p. 11, 2024, [Online]. Available: <https://jfs.nfsu.ac.in/index.php/nfsujfs/article/view/6/9>
- [22] A. Garg, L. K. Parmar, T. Garg, H. S. Dager, P. Bhardwaj, and A. Yadav, “Structural analysis and dielectric behavior of low-temperature synthesized nickel cobaltite,” *Chem. Phys. Impact*, vol. 8, no. September 2023, p. 100457, 2024, doi: 10.1016/j.chphi.2024.100457.
- [23] S. T. Navale et al., “Morphology engineering of hierarchical spinal nickel-cobaltite nanostructures for enhanced ethanol detection,” *Nano-Structures & Nano-Objects*, vol. 34, p. 100981, Apr. 2023, doi: 10.1016/j.nanoso.2023.100981.
- [24] Y. Tarpoudi Baheri and A. M. Homayounfard, “A review of synthesis strategies for nickel cobaltite-based composites in supercapacitor applications,” *Synth. Sinter.*, vol. 4, no. 1, pp. 41–53, Mar. 2024, doi: 10.53063/synsint.2024.41209.
- [25] M. Kaur, P. Chand, and H. Anand, “Binder free electrodeposition fabrication of NiCo₂O₄ electrode with improved electrochemical behavior for supercapacitor application,” *J. Energy Storage*, vol. 52, p. 104941, Aug. 2022, doi: 10.1016/j.est.2022.104941.
- [26] Y. M. Hunge, A. A. Yadav, S.-W. Kang, H. Kim, A. Fujishima, and C. Terashima, “Nanoflakes-like nickel cobaltite as active electrode material for 4-nitrophenol reduction and supercapacitor applications,” *J. Hazard. Mater.*, vol. 419, p. 126453, Oct. 2021, doi: 10.1016/j.jhazmat.2021.126453.
- [27] D. P. Dubal, P. Gomez-Romero, B. R. Sankapal, and R. Holze, “Nickel cobaltite as an emerging material for supercapacitors: An overview,” *Nano Energy*, vol. 11, pp. 377–399, Jan. 2015, doi: 10.1016/j.nanoen.2014.11.013.
- [28] N. Srivastava et al., “Microbial synthesis of nickel–cobaltite nanoparticle for biofuel applications,” in *Recent Developments in Bioenergy Research*, Elsevier, 2020, pp. 349–362. doi: 10.1016/B978-0-12-819597-0.00018-0.
- [29] A. Khorsand Zak, W. H. A. Majid, M. Ebrahimizadeh Abrishami, R. Yousefi, and R. Parvizi, “Synthesis, magnetic properties and X-ray analysis of Zn_{0.97}X_{0.03}O nanoparticles (X = Mn, Ni, and Co) using Scherrer and size–strain plot methods,” *Solid State Sci.*, vol. 14, no. 4, pp. 488–494, Apr. 2012, doi: 10.1016/j.solidstatesciences.2012.01.019.
- [30] A. Shabashini, S. Richard, M. K. Panda, S. K. Panja, and G. C. Nandi, “Real-time visualization of latent fingerprints with level 3 details based on a solid state emissive organic fluorophore using the powder dusting method,” *Mater. Adv.*, vol. 5, no. 3, pp. 1099–1105, 2024, doi: 10.1039/D3MA00870C.
- [31] S. Of and C. Vision, “Stereomicroscopic Gender Determination From Fingerprint Ridge Stereomicroscopic Gender Determination From Fingerprint Ridge Density and Fingerprint,” *Proc. 24th Myanmar Mil. Med. Conf.*, no. February, 2017.

- [32] H. Khmila, N. Smaoui, I. Khanfir, and H. Derbel, "An efficient method for the extraction of closed and open pores in fingerprint images," in 2019 16th International Multi-Conference on Systems, Signals & Devices (SSD), IEEE, Mar. 2019, pp. 154–157. doi: 10.1109/SSD.2019.8893238.
- [33] B. K. Sharma, R. Bashir, M. Hachem, and H. Gupta, "A comparative study of characteristic features of sweat pores of finger bulbs in individuals," Egypt. J. Forensic Sci., vol. 9, no. 1, p. 43, Dec. 2019, doi: 10.1186/s41935-019-0144-4.
- [34] M. K. Thakar and T. Sharma, "Digital grid method for fingerprint identification and objective report writing," Egypt. J. Forensic Sci., vol. 6, no. 2, pp. 194–201, Jun. 2016, doi: 10.1016/j.ejfs.2016.05.008.
- [35] I. T. Services, "Procedure for obtaining Biometric Device Certification (Authentication) STQC - IT Services," vol. 110003, no. 1, 2011.

Author Contributions

All authors listed on this manuscript have made substantial contributions to its creation and are accountable for all aspects of the work. Each author has participated in the following aspects of the research and manuscript preparation:

- **Conceptualization:** VB, SM
- **Methodology:** VB, SM
- **Investigation:** VB, HB, RR, SM
- **Formal Analysis:** VB, HB, RR, SM
- **Data Curation:** VB, SM
- **Writing - Original Draft:** VB, SM
- **Writing - Review & Editing:** VB, SM
- **Visualization:** VB, SM
- **Supervision:** SM

About the Authors

Vikash Bhadwa:

Vikash Bhadwa is a student at National Forensic sciences university (NFSU), Goa Campus and is currently pursuing his B.Sc. M. Sc. Forensic Science degree. He is a member of Multidisciplinary Research and Innovation Centre (MRIC), NFSU Goa.



Harshada Borude:

Harshada Borude belongs to NFSU, Goa Campus and is currently pursuing her B.Sc. M. Sc. Forensic Science degree. She is also a member of MRIC, NFSU Goa where She is pursuing research.



Riya Raj:

Riya Raj is currently doing her B.Sc. M.Sc. Forensic Science degree from NFSU, Goa Campus. She is also involved in research at MRIC, NFSU Goa.



Sandeep Munjal:

Sandeep Munjal completed his PhD in Physics from Indian Institute of Technology, Delhi. Currently he is an Assistant Professor at NFSU Goa Campus and the head of MRIC, NFSU Goa. His areas of research include novel materials for forensic applications and hardware security primitives

